Structural Determinants of Miscibility in Surface Films of Galactosylceramide and Phosphatidylcholine: Effect of Unsaturation in the Galactosylceramide Acyl Chain†

Shaukat Ali, Howard L. Brockman, and Rhoderick E. Brown*
The Hormel Institute, The University of Minnesota, Austin, Minnesota 55912
Received June 11, 1991; Revised Manuscript Received September 4, 1991

ABSTRACT: The Langmuir film balance technique has been used to define the surface structure and determine the mixing behavior of galactosylceramide (GalCer) and phosphatidylcholines in surface phases. To determine the effect of unsaturation on surface behavior, chain-pure GalCer species containing either oleoyl ($18{:}1^{\Delta 9}$), eicosenoyl ($20{:}1^{\Delta 11}$), or eicosadienoyl ($20{:}2^{\Delta 11,14}$) fatty acyl chains were synthesized. Using bovine brain GalCer as a reference, surface pressure versus molecular area (π–A) isotherms of the pure lipids were measured and analyzed by determining their compressibilities and by using an equation of state for lipid monolayers. This information, when coupled with surface potential versus molecular area (ΔV–A) analyses, provides insights into GalCer surface structure in terms of molecular packing and orientation. Lipid mixing behavior was determined by classical approaches which involve analyzing the average molecular area, the average surface dipole moment, and surface pressure as a function of film composition. The results indicate that, in contrast to the complex mixing behavior displayed by bovine brain GalCer and 1-palmitoyl-2-oleoyl-*sn*-glycero-3-phosphocholine (POPC), chain-pure GalCer species containing either oleoyl, eicosenoyl, or eicosadienoyl fatty acyl chains are miscible with POPC over the entire composition range. Moreover, increasing amounts of GalCer containing eicosenoyl acyl chains systematically elevate dipalmitoylphosphatidylcholine's (DPPC) liquid-expanded-to-liquid-condensed transition pressure. Such behavior is consistent with GalCer being miscible with the liquid-expanded phase of DPPC. Thus, fatty acyl unsaturation is a critical parameter governing the mixing behavior of GalCer with phosphatidylcholine.

Certain tissues (e.g., myelin, intestinal brush border epithelium, granular epidermis) contain significant amounts of monoglycosylceramides in their membranes. The relatively high concentrations are believed to fulfill specific physiochemical requirements necessary for the specialized functions of these membranes. In most other tissues, these glycosphingolipids (GSLs)[1] are minor membrane constituents. If membrane concentrations of monoglycosylceramides exceed optimum levels, as is the case in certain diseases (e.g., Krabbe's and Gaucher's diseases), membrane function is impaired (Gal et al., 1986). The molecular basis for such behavior is not well understood and has led to recent interest in the physicochemical properties of monoglycosylceramides as well as studies of their interactions with other membrane lipids such as cholesterol and phospholipids [for review, see Thompson and Tillack (1985) and Curatolo (1987)].

Like phospholipids, naturally occurring monoglycosylceramides possess acyl chain heterogeneity. However, the molecular nature of this heterogeneity is somewhat different from phospholipids. In cerebrosides isolated from brain tissue, the fatty acyl chains are relatively long, and a large fraction is hydroxylated (O'Brien & Rouser, 1964; DeVries & Norton, 1974). The physical consequences of such chemical characteristics have been investigated by a variety of biophysical approaches (Thompson & Tillack, 1985; Curatolo, 1987) including monolayer film balance techniques (Quinn & Sherman, 1971; Oldani et al., 1975; Maggio et al., 1978a; Ries, 1982; Johnston & Chapman, 1988). From these and other studies, it is clear that monoglycosylceramides behave quite differently than many other membrane lipids. Their unique chemical composition endows these lipids with the ability to form multiple inter- and intramolecular hydrogen bonds [for a review, see Boggs (1987)]. This makes for unusual properties that affect mixing with other lipids. For instance, in recent studies by Gardam and Silvius (1989) and by Jones et al. (1990), both groups noted that changing the fatty acyl chain length in monoglycosylceramides had little effect on their mixing behavior with dipalmitoylphosphatidylcholine (DPPC). Such findings imply that the headgroup and/or sphingoid base, not acyl chain length, are primarily responsible for inducing the phase separation that occurs in mixtures of monoglycosylceramides and DPPC. Unclear is whether introducing unsaturation into the acyl chains of monoglycosylceramides changes their physicochemical properties sufficiently to overcome the headgroup and/or sphingoid base interactions that appear to dominate their mixing behavior with phosphatidylcholines. Understanding the effect of acyl chain unsaturation on GalCer behavior is relevant to biological systems such as human plasma and unfertilized chicken egg yolks in which nearly 30% of the fatty acyl composition of GalCer is monounsaturated (Kundu, 1985; Li et al., 1978).

In the present investigation, we have utilized monolayer film balance techniques to characterize several homogeneously N-acylated galactosylsphingosines (GalSphs) as well as their mixing properties with 1-palmitoyl-2-oleoylphosphatidylcholine (POPC) and DPPC. Using the monolayer technique permits lipid mixing behavior to be studied systematically over the range of molecular areas known to occur in membrane systems while avoiding changes in lipid aggregation behavior that often

† This work was supported by USPHS Grant HL08214 and the Hormel Foundation.
* Address correspondence to this author at The Hormel Institute, The University of Minnesota, 801 16th Ave. N.E., Austin, MN 55912.

[1] Abbreviations: GSLs, glycosphingolipids; GalCer, galactosylceramide; GalSph, galactosylsphingosine; POPC, 1-palmitoyl-2-oleoylphosphatidylcholine; GalSpd, galactosylsphingoid; DPPC, dipalmitoylphosphatidylcholine; LE, liquid-expanded; LC, liquid-condensed.

0006-2960/91/0430-11198$02.50/0

occur in bulk model systems as lipid composition is varied. While this approach has been used to study the mixing behavior of many phospholipids and neutral lipids [for a review, see Dörfler (1990)], little has been reported for glycosphingolipid mixing with other lipids (Maggio et al., 1978b; Johnston & Chapman, 1988). This report focuses on the effects of introducing unsaturation into GalCer's fatty acyl chains. The results show that, in the absence of strong cohesive interactions between aliphatic moieties, GalCer and phosphatidylcholine are miscible in a nearly ideal manner. A preliminary report on portions of this work has appeared elsewhere (Ali et al., 1991).

Materials and Methods

Lipids. Bovine brain GalCer, POPC, and DPPC were purchased from Avanti Polar Lipids (Birmingham, AL). GalCer species containing homogeneous acyl chains were synthesized in the following way. Psychosine (galactosylsphingoid, GalSpd), obtained from natural GalCer by alkaline hydrolysis (Radin, 1974), was purified by medium-pressure flash column chromatography on silica gel (230–400 mesh) using step gradients consisting of $CHCl_3$, $CHCl_3/CH_3OH$ (9:1), and $CHCl_3/CH_3OH$ (1:1). Removal of GalSpd containing dihydrosphingosine from GalSpd containing sphingosine was accomplished by preparative thin-layer chromatography (TLC) (1-mm-thick plates; Analtech) using $CHCl_3/CH_3OH/NH_4OH$ (6:3:0.5). Normally, bovine brain GalCer contains less than 10% of the dihydrosphingosine base (Radin, 1974). The resulting galactosylsphingosine (GalSph) was N-acylated at room temperature using triphenylphosphine, aldrithiol, and the desired fatty acid (Kishimoto, 1975; Gardam & Silvius, 1989). After 6 h of reaction time, products were purified by flash column chromatography on silica gel (230–400 mesh) using step gradients of $CHCl_3$ (100 mL), $CHCl_3/CH_3OH$ (98:2, 100 mL), and $CHCl_3/CH_3OH$ (9:1, 300–400 mL). Final purification was achieved by preparative TLC using $CHCl_3/CH_3OH$ (85:15). Contaminating silica gel was removed by dissolving the GalCer in $CHCl_3/CH_3OH$ (5 mL) and eluting with CH_3OH through a C18 reverse-phase column equilibrated in CH_3OH (Kubo & Hoshi, 1985). Final yields of GalCer containing either oleoyl ($C18{:}1^{\Delta 9}$), eicosenoyl ($C20{:}1^{\Delta 11}$), or eicosadienoyl ($C20{:}2^{\Delta 11,14}$) acyl chains ranged from 30 to 50%.

The purity of each lipid was checked by TLC using different solvent systems. For detection of lipid impurities, two methods were used. Plates either were sprayed with 10% H_2SO_4 in 95% ethanol and charred on a hot plate maintained at 100 °C or were sprayed with the fluorescent dye primulin, which detects as little as 50 pmol of diacyl lipid (Kundu, 1982). GalCer purity was also analyzed using orcinol spray, which reacts with sugars. All lipids were judged to be greater than 99% pure. GalCer species were characterized by ^1H NMR. Characteristic peaks, recorded at 300 MHz (Varian Unity-300 NMR) in $CDCl_3/CD_3OD$ (2:1, v/v), were the following: δ 5.68–5.59 [1 H, dd, J = 7.4 and 15 Hz, C*H*(OH) = CH], 5.41–5.34 (1 H, dd, J = 7.4 and 15.2 Hz, CH = C*H*–R), 4.15 (1 H, d, J = 6.71 Hz, galactosyl H1′), 3.82 (1 H, d, J = 2.75 Hz, galactosyl H4′), 3.78–3.72 (1 H, dd, J = 6.71 and 11.59 Hz, *H*6′^{a}–H5′, H6′^{a}–H6′^{b}), 3.69–3.64 (1 H, dd, J = 4.89 and 11.60 Hz, galactosyl H6′^{b}–H5′, H6′^{b}–H6′^{a}), 2.15–2.10 (2 H, t, J = 8.01 Hz, C*H*$_2$CO), 0.85 (6 H, t, J = 6.66 Hz, ω-CH_3s). The fatty acyl chain composition of each GalCer species was over 99% pure as determined by GC–mass spectral analysis (Johnson and Brown, unpublished experiments).

After the lipids were dried overnight under P_2O_5 using a diffusion pump, stock solutions were prepared by dissolving in $CHCl_3/CH_3OH$/petroleum ether (5:1:4). Lipid concentrations were determined two ways. Aliquots of the stock solutions were placed on preweighed pans, dried by warming to 35 °C for 15 min, and immediately weighed using an analytical balance. In addition, stock concentrations were confirmed by chemical assays for nitrogen (Sloan-Stanley, 1967) or phosphate (Bartlett, 1959).

Solvents. Water was purified by reverse osmosis, mixed-bed deionization, adsorption on activated charcoal, and filtration through a 0.2-μm polycarbonate membrane (Nucleopore, Pleasanton, CA). Buffer was filtered through a Diaflo hollow fiber filter, degassed, and stored under argon. All other chemicals were of analytical grade and were purchased from Aldrich (Milwaukee, WI) or Sigma (St. Louis, MO).

Chloroform and methanol were distilled twice. Petroleum ether was purified as described by Smaby and Brockman (1985). Solvents were checked for surface-active impurities in two ways. In the first method, solvent aliquots (50–100 mL) were dried down and combined with a pure lipid standard (POPC), and the force–area isotherms were measured and compared with the known response of the lipid standard. Changes in the compression curve, particularly in the low-pressure region, as well as changes in the molecular area measured at film collapse, served as reliable indicators of surface impurities. In the second method, aliquots of solvent were applied directly to the argon–water interface. After standing at a large molecular area for 4 min to permit solvent evaporation from the interface, surface potential–area isotherms were recorded. Changes in surface potential upon compression served as an indicator of solvent purity (Smaby & Brockman, 1990).

Surface Balance Measurements. Monolayer experiments were carried out in a laboratory equipped with a filtered air supply. All glassware was acid-cleaned. Surface pressure was measured as a function of molecular area using a fully automated, computerized Langmuir film balance (Brockman et al., 1980, 1984). After being dissolved in $CHCl_3/CH_3OH$/petroleum ether (5:1:4), lipids were spread in 51.7-μL aliquots onto a Teflon trough filled with ~800 mL of buffer [10 mM potassium phosphate (pH 6.6) and 100 mM NaCl]. After standing at a large molecular area for 4 min to ensure complete evaporation of solvent, the films were compressed continuously at a rate of <4 Å^2 molecule^{-1} min^{-1}. Throughout the experiments, the subphase temperature was 24 ± 1 °C, and the trough was kept under argon. Calibration of the film balance was performed with lipid standards according to their equilibrium spreading pressures (Smaby & Brockman, 1990). Surface potential was measured as a function of molecular area using a ^{210}Po ionizing electrode (Brockman et al., 1980, 1984; Smaby & Brockman, 1990). Each sample was run at least twice to ensure isotherm reproducibility.

Analysis of Isotherms. Monolayer phase transitions between liquid-expanded and liquid-condensed phases or between monolayer and bulk phases were identified using a combination of second and third derivatives of π with respect to A as previously described (Brockman et al., 1980, 1984). The liquid-condensed to solid-condensed monolayer transition of DPPC, which shows an abrupt increase rather than a decrease in isotherm slope, was identified as a maximum in the second derivative of π with respect to A.

π–A data for single-component lipid monolayers were analyzed by their compressibility and by a surface solution equation of state for liquid-expanded films:

$$k = (-1/A)(dA/d\pi) \quad (1)$$

where A is the area per molecule (angstroms squared) at the

indicated surface pressures and π is the corresponding surface pressure in dynes per centimeter.

The equation of state (Wolfe & Brockman, 1988; Smaby & Brockman, 1991a) is

$$\pi = (qKT/\omega_1) \ln \{(1/f_1)[1 + \omega_1/(A_\pi - \omega_0)]\} \quad (2)$$

where K is Boltzmann's constant, ω_1 is the cross-sectional area of water (9.65 Å^2), f_1 is a lipid–water interaction parameter at the interface, ω_0 represents the cross-sectional area of the dehydrated lipid, and A_π is the total surface area divided by the number of lipid molecules present at each π. The scaling parameter q is correlated to f_1 and thus is not unique (Smaby & Brockman, 1991a) but does provide for accurate description of the data.

Although the entire range of liquid-expanded behavior should be amenable to analysis, in practice, data obtained near the high- and low-pressure limits may be particularly sensitive to trace impurities [e.g., see Middleton and Pethica (1981)] and the dynamics of the experiment. Thus, for reliable π–A data, the value at which $d^2\pi/dA^2$ goes from positive to negative (typically 10–20% below π_t) has been used as the upper limit, and the molecular area where π = 1.0 mN/m has been used as the lower limit (Smaby & Brockman, 1990).

Over the range of π noted above, the ΔV–A behavior of single-component liquid-expanded films is well described by

$$\Delta V = 37.7\mu_\perp/A + \Delta V_0 \quad (3)$$

where ΔV is the potential measured in millivolts and $\mu_\perp$ is the dipole moment (in milli-Debye) perpendicular to the lipid–water interface (Gaines, 1966) and is the slope of the ΔV versus $1/A$ plot. The intercept term, ΔV_0, is lipid-specific and appears to arise from the reorganization of interfacial water molecules during the transition from the gaseous to the liquid state (Smaby & Brockman, 1990).

Mixing behavior in two-component lipid monolayers was analyzed by different classical approaches. As shown by Crisp (1949a,b), construction of two-dimensional phase diagrams (transition pressure versus lipid composition) is often useful for determining whether or not the two components are miscible. Also, examination of the average molecular area, $\bar{A}$, as a function of lipid composition provides a way for detecting interactions among lipids. As shown by Goodrich (1957):

$$\bar{A} = A_1X_1 + A_2(1 - X_1) \quad (4)$$

where $\bar{A}$ is the average area in the mixed monolayer and x_1 is the mole fraction of the first lipid component. A_1 and A_2 are the mean molecular areas of the two pure components 1 and 2 at the same surface pressure. The extent of lipid mixing can be evaluated by deviations from simple additivity for $\bar{A}$.

Analogously, the behavior of the average surface potential ($\Delta\bar{V}$) as a function of lipid composition provides information about the mixing behavior of components [e.g., see Shah and Schulman (1968)]. Using eq 3, values for the surface dipole moment, $\mu_\perp$, of each pure component can be calculated from the slope of their ΔV versus $1/A$ plots. Ideal behavior can then be calculated at various lipid compositions based on additivity. Miller et al. (1987) have shown that, when liquid-expanded and liquid-condensed phase domains coexist, $\Delta\bar{V}$ apportions according to the area-weighted average of the surface potential of each phase. Recently, similar behavior has been observed for two component lipid mixtures that are ideally miscible (Smaby & Brockman, 1991b). The dipole moments of the experimental mixtures can then be determined from the slope of their $\Delta\bar{V}$ versus $1/A$ plots and compared with the ideal behavior based on additivity. Deviations from additivity indicate interactions between the components in the monolayer.

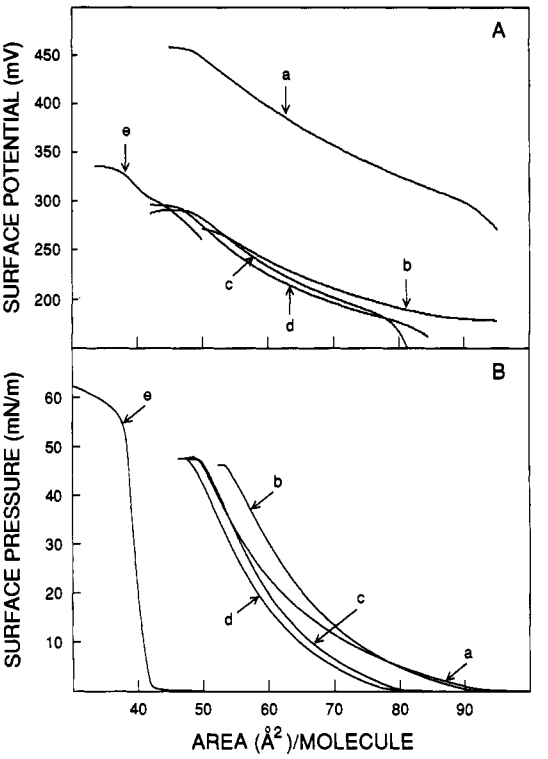

FIGURE 1: (A) Surface potential vs molecular area (ΔV–A) and (B) surface pressure vs molecular area (π–A) isotherms. Data were collected as described under Materials and Methods. (a) POPC, (b) N-20:2$^{\Delta 11,14}$ GalSph, (c) N-18:1$^{\Delta 9}$ GalSph, (d) N-20:1$^{\Delta 11}$, (e) bovine brain GalCer.

Table I: Lipid Compressibilities[a]

	π = 1.5 mN/m		π = 30 mN/m	
lipid species	A (Å^2)	k (×10^{-3} m/mN)	A (Å^2)	k (×10^{-3} m/mN)
POPC	90	30.3	56	8.3
N-20:1$^{\Delta 11}$ GalSph	75	20.7	54	6.2
N-18:1$^{\Delta 9}$ GalSph	79	21.2	57	6.0
N-20:2$^{\Delta 11,14}$ GalSph	87	22.9	61	6.8
bovine brain GalCer	42	3.3	40	1.3

[a] Compressibilities were calculated as described under Materials and Methods.

RESULTS

Galactosylceramide Isotherms. π–A isotherms of semisynthetic GalCer species containing oleoyl (18:1$^{\Delta 9}$), eicosenoyl (20:1$^{\Delta 11}$), or eicosadienyl (20:2$^{\Delta 11,14}$) fatty acyl chains are shown in Figure 1. For reference, the π–A isotherms of bovine brain GalCer and POPC are included. At 24 °C, GalCer isolated from bovine brain exhibits solid-condensed behavior. There is no hint of "lift-off" until a molecular area near 45 Å^2 is reached, and below 42 Å^2, the surface pressure rises steeply until a poorly defined collapse begins near 55 mN/m. The collapse pressure is compression rate dependent, increasing to over 60 mN/m when the compression rate is slowed to 3 Å^2 molecule^{-1} min^{-1}. Identical behavior is observed using three different spreading solvents. In contrast to bovine brain GalCer, POPC and all three unsaturated GalCer species produce liquid-expanded isotherms and compression rate has no effect on their collapse pressures. Interestingly, at any π, each of the unsaturated GalCer π-A isotherms is significantly less compressible than that of POPC, but all the unsaturated GalCer isotherms are similarly shaped. Comparison of the compressibilities is shown in Table I.

Table II: Physical Parameters Derived from the Isotherms[a]

lipid species	π_t	A_t	ω_0	f_1	$\mu_\perp$	ΔV_0
N-18:1$^{\Delta 9}$ GalSph	46.9	51.5	42.2	1.258	365	6.03
N-20:1$^{\Delta 11}$ GalSph	47.2	49.7	39.9	1.259	343	12.01
N-20:2$^{\Delta 11,14}$ GalSph	46.1	55.8	45.3	1.215	299	51.5
native GalCer	56.9	39.4	37.5	3.098	270	60.5
POPC	47.3	51.9	39.7	1.172	465	115.5

[a] Error ~±4%. π_t is the collapse pressure. A_t is the collapse area. Other parameters were calculated as described under Materials and Methods.

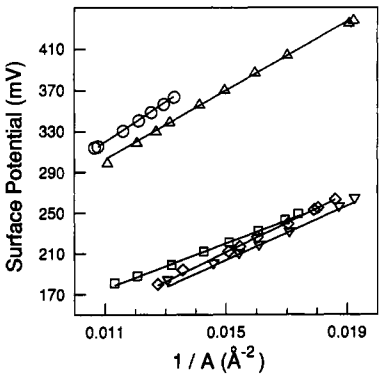

FIGURE 2: Surface potential vs inverse molecular area. Data were collected as described under Materials and Methods. (○) DPPC, (△) POPC, (□) N-20:2$^{\Delta 11,14}$ GalSph, (◇) N-18:1$^{\Delta 9}$ GalSph, (▽) N-20:1$^{\Delta 11}$ GalSph.

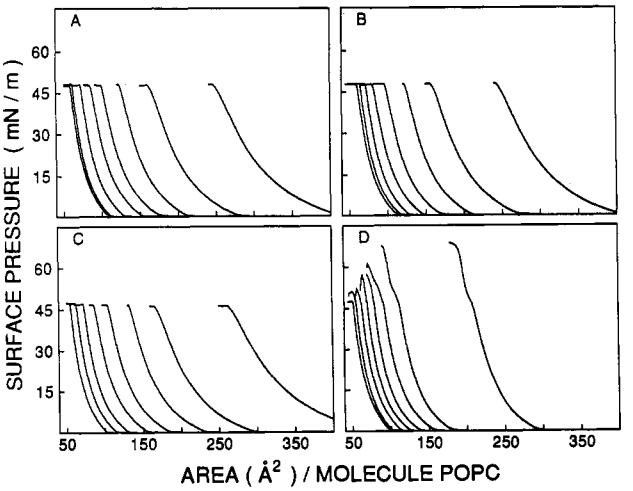

FIGURE 3: Surface pressure vs molecular area of GalCer and POPC mixtures. The molecular area is normalized to the molecules of POPC in the films. In each panel, isotherms (from left to right) show the effect of 0.1 incremental increases in the mole fraction of GalCer starting at 0.1 and ending at 0.8. (A) POPC and N-18:1$^{\Delta 9}$ GalSph, (B) POPC and N-20:1$^{\Delta 11}$ GalSph, (C) POPC and N-20:2$^{\Delta 11,14}$ GalSph, (D) POPC and bovine brain GalCer.

Even though the isotherms for each unsaturated GalCer species are very similarly shaped, each curve possesses subtle differences that reflect the structural changes imparted by each fatty acyl chain. For instance, N-18:1$^{\Delta 9}$ GalSph's collapse pressure and area are very similar to those of POPC. However, the "lift-off" area of N-18:1$^{\Delta 9}$ GalSph is significantly smaller than that of POPC. Increasing the acyl chain length of GalCer by two carbons (20:1$^{\Delta 11}$) results in a similar collapse pressure but a smaller collapse area as well as smaller "lift-off" area compared to N-18:1$^{\Delta 9}$ GalSph. Introducing a second double bond into the fatty acyl chain (20:2$^{\Delta 11,14}$) of GalCer shifts the "lift-off" and collapse areas to larger values while slightly lowering the collapse pressure.

Other structural parameters are revealed by analyzing the isotherms (Figure 1B) with an equation of state for monolayers (Wolfe & Brockman, 1988; Smaby & Brockman, 1991a). This equation of state has been shown to be valid for several different lipids displaying liquid-expanded film behavior (see Materials and Methods). Resulting values for the area at collapse (A_t) and the limiting molecular areas (ω_0) for each unsaturated GalCer species as well as the POPC and bovine brain GalCer reference compounds are shown in Table II. In general, the values are consistent with the structural alterations induced by the changes in fatty acyl structure.

To determine the interfacial orientation of each unsaturated GalCer species, the surface potential was measured as a function of molecular area (Figure 1A). POPC and bovine brain GalCer were used as references. In general, the ranges [N-18:1$^{\Delta 9}$ GalCer (185–290 mV), N-20:1$^{\Delta 11}$ GalCer (190–295 mV), N-20:2$^{\Delta 11,14}$ GalCer (195–270 mV)] were considerably lower than bovine brain GalCer (300–325 mV) and dramatically lower than POPC (290–460 mV). Interestingly, at a given molecular area in the liquid-expanded isotherms, ΔV of each unsaturated GalCer species is within 20 mV of one another, but the absolute values are 40–50% lower than that observed for POPC.

Within the practical range of liquid-expanded behavior, plots of ΔV versus $1/A$ are generally linear (Figure 2). Although such behavior has been reported for several glycerol-based lipids and long-chain acyl derivatives (Smaby & Brockman, 1990), only one sphingolipid was examined. From such plots, it is clear that linear behavior is observed for the unsaturated GalCer species. The slope of these plots can be used to estimate the perpendicular component of the dipole moment in the sphingolipids. Additionally, each of the unsaturated GalCer species possesses a characteristic constant potential term, ΔV_0. These constants appear to be a consequence of the reorganization of interfacial water molecules by the lipid that occurs as the liquid-expanded state forms and depend directly on the physicochemical properties of the lipid (Smaby & Brockman, 1990; Yokoyama & Kézdy, 1991).

Mixed Films of Semisynthetic GalCer Species and POPC. Figure 3 shows representative isotherms of binary mixtures of POPC and chain-pure N-acylated GalSph containing either oleoyl (Figure 3A), eicosenoyl (Figure 3B), or eicosadienoyl (Figure 3C) residues. The surface pressure (π) is plotted as a function of the apparent molecular area of POPC. With increasing mole fraction of each GalCer species, an expansion of the apparent molecular area of POPC occurs. At a given mole fraction, the expansion is greater with N-20:2$^{\Delta 11,14}$ GalSph than with either N-19:1$^{\Delta 9}$ GalSph or N-20:1$^{\Delta 11}$ GalSph, which have nearly identical effects on the POPC area. In contrast, bovine brain GalCer produces decidely less expansion of the POPC than any of the unsaturated GalCer species.

To characterize the mixing behavior of the unsaturated GalCer species with POPC at different surface pressures, plots of the average molecular area ($\bar{A}$) versus composition (Figure 4) were constructed at three different surface pressures (1, 22, and 45 mN/m). The solid lines represent ideal additivity calculated using eq 4 (see Materials and Methods). As a reference, the mixing behavior of bovine brain GalCer and

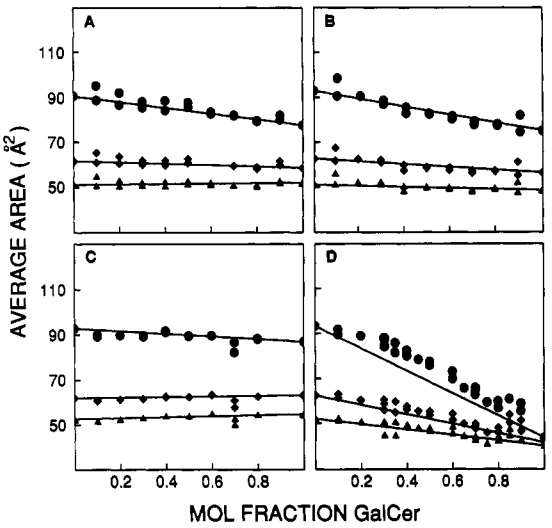

FIGURE 4: Average molecular area vs composition. In each panel: (●) 1 mN/m; (♦) 22 mN/m; (▲) 45 mN/m. (A) POPC and *N*-18:1$^{\Delta 9}$ GalSph, (B) POPC and *N*-20:1$^{\Delta 11}$ GalSph, (C) POPC and *N*-20:2$^{\Delta 11,14}$ GalSph, (D) POPC and bovine brain GalCer. Ideal area additivity is represented by the solid line.

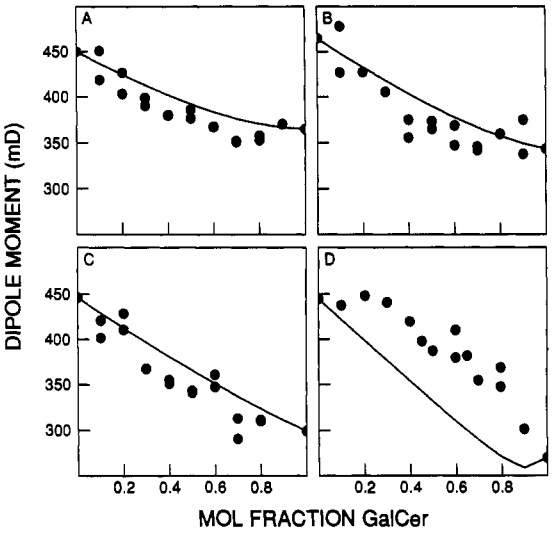

FIGURE 5: Average dipole moment vs lipid composition. Average dipole moments were calculated from the average surface potential data as described under Materials and Methods. In each panel, ideal additivity is based on apportionment of the dipole moment of the pure lipids according to their molecular areas and is represented by the solid line. (A) POPC and *N*-18:1$^{\Delta 9}$ GalSph, (B) POPC and *N*-20:1$^{\Delta 11}$ GalSph, (C) POPC and *N*-20:2$^{\Delta 11,14}$ GalSph, (D) POPC and bovine brain GalCer.

POPC is included (Figure 4D). Interestingly, at 1, 22, or 45 mN/m, $\bar{A}$ for any of the unsaturated GalCer species mixed with POPC behaves as predicted by the additive areas of pure components across the entire compositional range (Figure 4A–C). $\bar{A}$ value for the *N*-18:1$^{\Delta 9}$ GalSph–POPC and the *N*-20:1$^{\Delta 11}$ GalSph–POPC mixtures with increasing GalCer content are nearly identical when mole fractions and surface pressure are the same. Not surprisingly, *N*-20:2$^{\Delta 11,14}$ GalSph–POPC mixtures show slightly larger $\bar{A}$ values as the mole fraction of *N*-20:2$^{\Delta 11,14}$ GalSph increases. This effect is most evident at 1 mN/m. In contrast, $\bar{A}$ values of the bovine brain GalCer–POPC mixtures show positive deviations from area additivity at both 1 and 22 mN/m. The deviation increases as the GalCer content rises from zero to 30 mol % and remains constant between 30 and 60 mol% before gradually returning to area additivity. The presence of miscibility gaps, similar to those reported by Matuo et al. (1981, 1982a,b) for other mixtures of solid-condensed and liquid-expanded lipids, adds to the complexity of the data. Although none of the mixtures of POPC and the unsaturated GalCer species possess such miscibility gaps, the ideal additivity displayed in the $\bar{A}$ behavior could be due to either ideal miscibility or immiscibility.

Crisp (1949a,b) has pointed out that clear distinction between miscibility and immiscibility in surface phases can generally be made by applying the phase rule and constructing two-dimensional phase diagrams. The reference mixture of bovine brain GalCer and POPC illustrates how such distinctions can be made. Using the data in Figure 3D, surface pressure transition versus composition phase diagrams can be constructed (data not shown). At low GalCer compositions (0–30 mol %), isotherms are smooth and continuous without inflections or discontinuities and show a progressive increase in the surface pressure required to collapse the films. Such behavior suggests that bovine brain GalCer and POPC are miscible within this compositional range. At higher bovine brain GalCer compositions (30–80 mol %), complex isotherms with high collapse pressures and with apparent transitions that change as a function of composition are observed. Although such behavior can be explained as regions of immiscibility, other factors such as film metastability and kinetic restrictions on mixing of condensed lipids (Cadenhead et al., 1976) complicate clear interpretation, especially of the GalCer-rich regions of the phase diagram. No such complications exist for the unsaturated GalCer species (Figure 3). However, because the collapse pressures of the unsaturated GalCer species are so similar to that of POPC (Table II), in practice, such analysis provides no real insight into the mixing behavior.

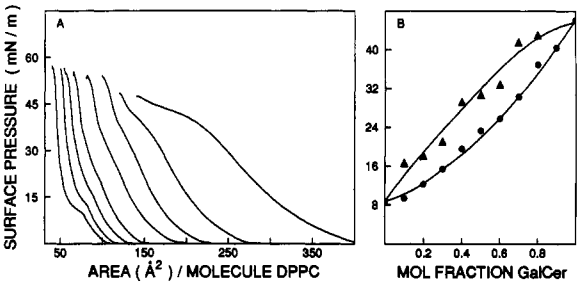

FIGURE 6: Effect of increasing amounts of GalCer on the liquid-expanded to liquid-condensed transition of DPPC. Transitions were identified as described under Materials and Methods. (A) The molecular area is normalized to the molecules of DPPC in the films. Isotherms (from left to right) show the effect of 0.1 incremental increases in the mole fraction of *N*-20:1$^{\Delta 11}$ GalSph starting at 0.1 and ending at 0.8. (B) Liquid-expanded to liquid-condensed transitions are represented by (●). Liquid-condensed to solid-condensed transitions are represented by (▲).

An alternative but seldom used way to gain insight into lipid mixing behavior is to make use of the surface potential (ΔV) data that are accessible by the monolayer approach. This approach is informative because, at equivalent molecular areas, ΔV of POPC is nearly 100 mV higher than that of each unsaturated GalCer derivative (Figures 1 and 2). Figure 5 shows that the average dipole moment for each of the mixtures containing unsaturated GalCer (Figure 5A–C) deviates from ideal additivity in a slightly negative way. This behavior suggests that each of the unsaturated GalCer species is miscible with POPC in a slightly nonideal manner. In contrast, the average dipole moment of the bovine brain GalCer–POPC mixtures deviates from additivity in a markedly positive fashion above 20 mol % GalCer.

To confirm this miscibility of the unsaturated GalCer species in liquid-phase phosphatidylcholines, a final test was undertaken. In this experiment, the effect of increasing amounts

of *N*-20:1$^{\Delta 11}$ GalCer on the liquid-expanded-to-liquid-condensed transition of DPPC at 24 °C was monitored. Figure 6A shows that increasing mole fractions of this unsaturated GalCer species elevate the surface pressure of DPPC's LE-to-LC transition. A plot of the transition pressures versus composition is shown in Figure 6B (lower curve). The behavior strongly suggests that *N*-20:1$^{\Delta 11}$ GalSph is miscible with the liquid-expanded phase of DPPC. Interestingly, similar behavior is observed for a condensed-state transition (Figure 6B; upper curve) and suggests that *N*-20:1$^{\Delta 11}$ GalSph is also miscible with liquid-condensed DPPC.

Discussion

The goal of this study was to determine to what extent headgroup interactions dominate the mixing behavior of phosphatidylcholine and galactosylceramide. Previously, Gardam and Silvius (1989) and Jones et al. (1990) noted that changing the fatty acyl chain length in monoglycosylceramides had little effect on their mixing behavior with DPPC. The implication of these studies was that the headgroup and/or sphingoid base, not the fatty acyl chain length, is primarily responsible for inducing the phase separation that occurs at certain mixing ratios of monoglycosylceramides and DPPC. Yet, to what extent structural modifications to the cerebroside acyl chain (e.g., unsaturation) can change their mixing behavior with phosphatidylcholines is not known. Thus, we have initiated a rigorous analysis of glycosphingolipid and phospholipid mixing behavior in surface behaviors to identify structural parameters responsible for modifying mixing behavior.

Structure of Galactosylceramide Monolayers. Prior to studying the mixing behavior of unsaturated GalCer and phosphatidylcholines in surface films, a basic characterization of the unsaturated GalCer species was undertaken using a Langmuir film balance. Of the previous monolayer studies involving GalCer (Quinn & Sherman, 1973; Oldani et al., 1975; Maggio et al., 1978a; Ries, 1982; Johnston et al., 1985; Fidelio et al., 1986), most have focused on bovine brain GalCer, which contains primarily long, saturated acyl chains and their 2-hydroxy derivatives. Two of these studies also included π–A isotherms of *N*-palmitoyl GalSpd (Oldani et al., 1975; Maggio et al., 1978a), and one recent study included π–A isotherms of GalCer containing stearoyl, oleoyl, and nervonyl acyl chains (Johnston & Chapman, 1988). Although difficult to compare because of differences in experimental conditions, our results are in general agreement with those of Johnston and Chapman (1988), who reported that *N*-oleoyl GalSpd forms liquid-expanded films on a subphase of pure water at 37 °C. We found that GalCer containing either oleoyl, eicosenoyl, or eicosadienoyl acyl chains forms liquid-expanded films at 24 °C on a phosphate-buffered saline subphase (Figure 1). Interestingly, each of these π–A isotherms is similarly shaped but has a more limited range of compressibility than POPC, which also produces a liquid-expanded isotherm. This is the case not only for *N*-oleoyl and *N*-eicosenoyl GalSph which contain one cis double bond in the middle of their acyl chains but also for *N*-eicosadienoyl GalSph which contains two cis double bonds (Δ11 and Δ13). It appears unlikely that intermolecular hydrogen bonding between the polar regions of the unsaturated GalCer molecules is responsible for the reduced compressibility. The expansivity induced by the unsaturated acyl chains is sufficiently large so as to preclude appropriate ordering between adjacent molecules and thereby prevent the dehydration of tightly bound interfacial water that probably must take place for intermolecular hydrogen bonding to occur. Indeed, the potential for GalCer and other sphingolipids to form intermolecular hydrogen bonds is well recognized [for review, see Boggs (1987), Curatolo (1987), and Thompson and Tillack (1985)]. However, intermolecular hydrogen bonding has only been clearly demonstrated for aqueous dispersions of GalCer molecules when they are in the gel state (Bunow & Levin, 1980; Lee et al., 1986; Pink et al., 1988).

Rather, the diminished lateral compressibility, especially at low surface pressures, must be attributed to the hydration of the polar region in the unsaturated GalCer species which is almost certainly lower than that of POPC at 24 °C. Indeed, abundant evidence indicates that, when mixed with excess water, GalCer and certain monoglycosylglycerolipids are less hydrated than phosphatidylcholines [e.g., see Ruocco and Shipley (1983), Weislander et al. (1978), and Sen and Hui (1988)].

The similarity in the surface behavior of the unsaturated GalCer species is also reflected in their surface potentials (Figures 1 and 2). These results indicate that their average orientation is similar during compression. Compared to POPC, however, both the net change during compression and the absolute value of ΔV at a given molecular area are diminished. The large difference in the absolute value of ΔV at a given molecular area reflects inherent differences in the net dipoles of GalCer and POPC. Although it is tempting to attribute such differences to POPC's charged, zwitterionic, phosphorylcholine headgroup compared to GalCer's uncharged sugar headgroup, this probably is not the case. On the basis of surface potential measurements of phospholipids, it appears likely that phosphorylcholine's contribution to the surface potential would be relatively small because of charge shielding by counterions in the buffer and dipole compensation by the hydration shell (Beitinger et al., 1989; Miller et al., 1987). Rather, the structural differences of POPC's interfacial region, with a large perpendicular dipole component due to two ester-linked carbonyl groups, compared to GalCer's single amide-linked carbonyl group (and one hydroxyl group) is a more feasible explanation. In fact, Shah and Schulman (1967) have shown that the surface potential of sphingomyelin is much smaller than that of DPPC.

Although the compressibilities of the unsaturated GalCer species are all similar, clear differences exist in their liquid-expanded π–A isotherms. These differences are consistent with the structural changes associated with the different acyl chains. For instance, compared to *N*-oleoyl GalSph, the molecular area of *N*-eicosenoyl GalSph is about 4 Å^2 larger at 30 mN/m. This behavior is consistent with the rise in van der Waal's attractive forces caused by increasing acyl chain length (Salem, 1962). In contrast, introduction of a second cis double bond (*N*-eicosadienoyl GalSph) results in an increase in molecular area of about 7 Å^2 (at 30 mN/m) compared to *N*-eicosenoyl GalSph. Again, such behavior is consistent with the large decline in van der Waal's attractive forces known to accompany relatively small increases in average interchain distances (Salem, 1962). Introduction of the second cis double bond produces a second "kink" in the acyl chain. To minimize "free volume", which is energetically unfavorable, and to maximize interchain interactions, an increase in gauche rotomers occurs in the single carbon bonds adjacent to the rigid double bond [for a review, see Thompson and Huang (1986)]. The resulting average area increase produced by *N*-eicosadienoyl GalSph is consistent with this explanation.

The subtle changes in π–A isotherms resulting from the structural changes in the fatty acyl chain of GalCer are supported by calorimetric studies of hydrated bulk dispersions of

GalCer in which the thermotropic effects on increasing unsaturation in the fatty acyl region were measured (Reed & Shipley, 1989). As with phosphatidylcholines (Keough et al., 1987; Coolbear et al., 1983), increasing the number of cis double bonds from 0 to 1 and from 1 to 2 significantly decreases the phase transition temperature.

The liquid-expanded behavior of the unsaturated GalCer species is in marked contrast to that of bovine brain GalCer, which displays solid-condensed isotherms and a higher collapse pressure and higher surface potential. This behavior is generally consistent with previously published monolayer data (Quinn & Sherman, 1973; Oldani et al., 1975; Maggio et al., 1978a; Ries, 1982; Fidelio et al., 1986; Johnston et al., 1985). Subtle differences that do occur are probably the result of differing experimental conditions as well as variability in bovine brain GalCer fatty acyl composition known to occur with animal age (Svennerholm & Stallberg-Stenhagen, 1968). Bovine brain GalCer's solid-condensed π–A isotherm and high collapse pressure are undoubtedly a consequence of strong van der Waal's attractive forces between the long, predominantly saturated hydrocarbon and often 2-hydroxylated hydrocarbon chains (Jackson et al., 1988; Pink et al., 1988), the relatively low hydration shell of the neutral galactosyl headgroup (Ruocco & Shipley, 1983), and the favorable hydrogen-bonding conditions involving the sphingoid base and/or sugar headgroup (Pascher & Sundell, 1977; Bunow & Levin, 1980; Curatolo, 1985; Lee et al., 1986; Pink et al., 1988).

Mixed Monolayers of GalCer and PC. GalCer's containing oleoyl, eicosenoyl, or eicosadienoyl acyl chains are miscible with liquid-expanded phosphatidylcholines at 24 °C over the entire compositional range in surface films. Miscibility with DPPC is strongly suggested by the manner in which increasing mole fractions of *N*-eicosenoyl GalSph affect DPPC's liquid-expanded-to-liquid-condensed transition (Figure 6A). The transition pressure steadily rises with increasing *N*-eicosenoyl GalSph content, indicating that this unsaturated GalCer species is miscible with the liquid-expanded DPPC (lower curve in Figure 6B). Interestingly, similar behavior is also observed for a condensed-state transition (upper curve in Figure 6B). This behavior suggests that *N*-eicosenoyl GalSph is also miscible with liquid-condensed DPPC. The shapes of the transition pressure versus composition plots show the classic "cigar-shaped" behavior which generally is taken to mean ideal miscibility (Matuo et al., 1981, 1982a,b).

Miscibility of all the unsaturated GalCer species and POPC is evident from analysis of the average dipole moment versus composition behavior that can be derived from ΔV–A isotherms. Interestingly, the experimental points show only slight negative deviation from ideal additivity, suggesting that the components are miscible. This negative deviation from ideality contrasts with the findings of Maggio et al. (1978b), who reported positive deviations compared to additivity of the mean surface potential per molecule at 30 mN/m and 20 °C when either ceramide, glucosylceramide, or gangliotetraosylceramide (prepared from bovine brain gangliosides) were mixed with an equimolar amount of DPPC in surface films. However, we also noted positive deviations from ideality with equimolar bovine brain GalCer and POPC (Figure 5D).

Even though the average molecular area and transition pressure versus composition analyses, two classical approaches for analyzing two-component monomolecular films, provide only limited information about the mixing behavior of the unsaturated GalCer species and POPC, they are useful for understanding bovine brain GalCer and POPC mixing behavior. These lipids do show positive deviations from ideality in their $\bar{A}$ behavior at 1 and 22 mN/m (Figure 4D). Maggio et al. (1978b) also reported positive deviations in $\bar{A}$ when glucosylceramide (prepared from bovine brain gangliosides) is mixed with DPPC (30 mN/m, 20 °C). More recently, Johnston and Chapman (1988) measured $\bar{A}$ of bovine brain choline phosphatide and bovine brain GalCer mixed monolayers at 37 °C and at 2, 10, and 35 mN/m. They found positive deviations in $\bar{A}$ at all surface pressures regardless of whether non-hydroxy or 2-hydroxy fatty acyl chains were present in the GalCer. Although neither of these earlier studies included two-dimensional phase diagrams, our analysis of such data suggests that bovine brain GalCer and POPC are miscible when the GalCer mole fraction is below 0.35. Above this, multiple transitions are evident in the surface films (Figure 3D), which, although admittedly difficult to clearly define, may be due to partial immiscibility (35–80 mol %) or regions of metastability. Interestingly, evidence for immiscibility in this compositional range for hydrated bulk dispersions of bovine brain GalCer and POPC is evident from calorimetric and fluorometric studies (Curatolo, 1986; Bunow & Levin, 1988; Rintoul & Welti, 1989) as well as by recent freeze–fracture electron microscopic techniques which reveal a distinct ripple phase between 35 and 80 mol % GalCer (W. A. Anderson, S. B. Johnson, and R. E. Brown, unpublished experiments).

Implications. The present studies shed light on the structural parameters governing the mixing behavior of simple glycosphingolipids and phosphatidylcholines. Whereas the headgroup sugars and sphingoid backbone are known to be important in governing their mixing behavior, less attention has been paid to the effect of the fatty acid residue. Our results clearly show that structural alterations that increase the average molecular interfacial cross-sectional area, such as introduction of unsaturation in the fatty acyl chain of GalCer, can modulate the headgroup and/or sphingoid base interactions that impart cerebrosides with their unusual mixing properties with phosphatidylcholines. On the basis of the behavior of other lipid derivatives, one would also expect similar modulations to be produced if GalCer contains short, saturated acyl chains (e.g., C8:0–C12:0). The role of modulations in glycosphingolipid and phospholipid mixing behavior in regulating the activity of a lipid-transfer protein that is specific for glycolipids (Brown et al., 1985, 1990) is currently under investigation in this laboratory.

ACKNOWLEDGMENTS

We thank Jan Smaby for assistance with the monolayer experiments involving bovine brain GalCer, Susan Johnson for verifying the acyl chain homogeneity of the unsaturated GalCer species by GC–MS, Carmen Perleberg and Kerry Ruck for secretarial services, and cores A, C, and D of USPHS Program Project Grant HL08214 for drawing figures and use of the NMR and GC–MS equipment, respectively.

REFERENCES

Ali, S., Brockman, H. L., Johnson, S. B., Smaby, J. M., & Brown, R. E. (1991) *Biophys. J. 59*, 628a.

Bartlett, G. R. (1959) *J. Biol. Chem. 234*, 466–469.

Beitinger, H., Vogel, V., Mobius, D., & Rahmann, H. (1989) *Biochim. Biophys. Acta 984*, 293–300.

Boggs, J. M. (1987) *Biochim. Biophys. Acta 906*, 353–404.

Brockman, H. L., Jones, C. S., Schwebke, C. J., Smaby, J. M., & Jarvis, D. E. (1980) *J. Colloid Interface Sci. 78*, 502–512.

Brockman, H. L., Smaby, J. M., & Jarvis, D. E. (1984) *J. Phys. E.: Sci. Instrum. 17*, 351–353.

Brown, R. E., Stephenson, F. A., Markello, T., Barenholz, Y., & Thompson, T. E. (1985) *Chem. Phys. Lipids 38*, 79–93.
Brown, R. E., Jarvis, K. L., & Hyland, K. J. (1990) *Biochim. Biophys. Acta 1044*, 77–83.
Bunow, M. R., & Levin, I. W. (1980) *Biophys. J. 32*, 1007–1022.
Bunow, M. R., & Levin, I. W. (1988) *Biochim. Biophys. Acta 939*, 577–586.
Cadenhead, D. A., Kellner, B. M. J., & Phillips, M. C. (1976) *J. Colloid Interface Sci. 57*, 224–227.
Coolbear, K. P., Berde, C. B., & Keough, K. M. W. (1983) *Biochemistry 22*, 1466–1473.
Crisp, D. J. (1949a) in *Surface Chemistry*, pp 17–22, Butterworths, London.
Crisp, D. J. (1949b) in *Surface Chemistry*, pp 23–25, Butterworths, London.
Curatolo, W. (1982) *Biochemistry 21*, 1761–1764.
Curatolo, W. (1986) *Biochim. Biophys. Acta 861*, 373–376.
Curatolo, W. (1987) *Biochim. Biophys. Acta 906*, 111–136.
DeVries, G. H., & Norton, W. T. (1974) *J. Neurochem. 22*, 251–257.
Dörfler, H. D. (1990) *Adv. Colloid Interface Sci. 31*, 1–110.
Fidelio, G. D., Maggio, B., & Cumar, F. A. (1986) *Biochim. Biophys. Acta 854*, 231–239.
Gaines, G. L., Jr. (1966) *Insoluble Monolayers at Liquid/Gas Interfaces*, pp 73–89, Wiley-Interscience, New York.
Gal, A. E., Weis, A. L., Quirk, J. M., Tokoro, T., & Brady, R. O. (1986) *Chem. Phys. Lipids 42*, 199–207.
Gardam, M., & Silvius, J. R. (1989) *Biochim. Biophys. Acta 980*, 319–325.
Goodrich, F. C. (1957) *Proceedings of the 2nd International Congress of Surface Activity*, Vol. I, Butterworths, London.
Jackson, M., Johnston, D. S., & Chapman, D. (1988) *Biochim. Biophys. Acta 944*, 497–506.
Johnston, D. S., & Chapman, D. (1988) *Biochim. Biophys. Acta 937*, 10–22.
Johnston, D. S., Coppard, E., & Chapman, D. (1985) *Biochim. Biophys. Acta 815*, 325–333.
Jones, J. D., Almeida, P. F., & Thompson, T. E. (1990) *Biochemistry 29*, 70–76.
Keough, K. M. W., Giffin, B., & Kariel, N. (1987) *Biochim. Biophys. Acta 902*, 1–10.
Kishimoto, Y. (1975) *Chem. Phys. Lipids 15*, 33–36.
Kubo, H., & Hoshi, M. (1985) *J. Lipid Res. 26*, 638–641.
Kundu, S. (1981) *Methods Enzymol. 72*, 185–204.
Kundu, S., Diego, I., Osovitz, S., & Marcus, D. (1985) *Arch. Biochem. Biophys. 238*, 388–400.
Lee, D. C., Miller, I. R., & Chapman, D. (1986) *Biochim. Biophys. Acta 859*, 266–270.
Li, S.-C., Chien, J.-L., Wan, C., & Li, Y.-T. (1978) *Biochem. J. 173*, 697–699.
Maggio, B., Cumar, F. A., & Caputto, R. (1978a) *Biochem. J. 171*, 559–565.
Maggio, B., Cumar, F. A., & Caputto, R. (1978b) *Biochem. J. 175*, 1113–1118.
Matuo, H., Motomura, K., & Matuura, R. (1981) *Chem. Phys. Lipids 28*, 385–397.
Matuo, H., Motomura, K., & Matuura, R. (1982a) *Chem. Phys. Lipids 30*, 353–365.
Matuo, H., Rice, D. K., Balthasar, D. M., & Cadenhead, D. A. (1982b) *Chem. Phys. Lipids 30*, 367–380.
Middleton, S. R., & Pethica, B. A. (1981) *Faraday Symp. Chem. Soc. 16*, 109–123.
Miller, A., Helm, C. A., & Möhwald, H. (1987) *J. Phys. (Paris) 48*, 693–701.
O'Brien, J. S., & Rouser, G. (1964) *J. Lipid Res. 5*, 339–342.
Oldani, D., Hauser, H., Nichols, B. W., & Phillips, M. C. (1975) *Biochim. Biophys. Acta 382*, 1–9.
Pascher, I., & Sundell, S. (1977) *Chem. Phys. Lipids 20*, 175–191.
Pink, D. A., MacDonald, A. L., & Quinn, B. (1988) *Chem. Phys. Lipids 47*, 83–95.
Quinn, P. J., & Sherman, W. R. (1971) *Biochim. Biophys. Acta 233*, 734–752.
Radin, N. S. (1974) *Lipids 9*, 358–360.
Reed, R. A., & Shipley, G. G. (1989) *Biophys. J. 55*, 281–292.
Ries, H. E., Jr. (1982) *J. Colloid Interface Sci. 88*, 298–301.
Rintoul, D. A., & Welti, R. (1989) *Biochemistry 28*, 26–31.
Ruocco, M. J., & Shipley, G. G. (1983) *Biochim. Biophys. Acta 735*, 305–308.
Salem, L. (1962) *J. Chem. Phys. 37*, 2100–2113.
Sen, A., & Hui, S.-W. (1988) *Chem. Phys. Lipids 49*, 179–184.
Shah, D. O., & Schulman, J. H. (1967) *Lipids 2*, 21–27.
Shah, D. O., & Schulman, J. H. (1968) *Adv. Chem. Ser. 84*, 189–209.
Sloan-Stanley, G. H. (1967) *Biochem. J. 104*, 293–295.
Smaby, J. M., & Brockman, H. L. (1985) *Biophys. J. 48*, 701–708.
Smaby, J. M., & Brockman, H. L. (1990) *Biophys. J. 58*, 195–204.
Smaby, J. M., & Brockman, H. L. (1991a) *Langmuir 7*, 1031–1034.
Smaby, J. M., & Brockman, H. L. (1991b) *Langmuir* (in press).
Svennerholm, L., & Stallberg-Stenhagen, S. (1968) *J. Lipid Res. 9*, 215–225.
Thompson, T. E., & Tillack, T. W. (1985) *Annu. Rev. Biophys. Biophys. Chem. 14*, 361–386.
Thompson, T. E., & Huang, C. (1986) in *Membrane Physiology* (Andreoli, T. E., Hoffman, J. F., Fanestil, D. D., & Schultz, S. G., Eds.) 2nd ed., pp 25–44, Plenum Publishing, New York.
Weislander, A., Ulmius, J., Lindblom, G., & Fontell, K. (1978) *Biochim. Biophys. Acta 512*, 241–253.
Wolfe, D. H., & Brockman, H. L. (1988) *Proc. Natl. Acad. Sci. U.S.A. 85*, 4285–4289.
Yokoyama, S., & Kezdy, F. J. (1991) *J. Biol. Chem. 266*, 4303–4308.